High-order nonlinear susceptibilities of helium

Wei-Chih Liu*
Electron and Optical Physics Division, National Institute of Standards and Technology, Gaithersburg, Maryland 20899 and Institute for Physical Science and Technology, University of Maryland, College Park, Maryland 20742
(Received 12 May 1997)

With the goal of providing critically evaluated atomic data for modeling high harmonic generation processes in noble gases, we present calculations of frequency-dependent nonlinear susceptibilities of the ground state of helium, within the framework of Rayleigh-Schrödinger perturbation theory at lowest applicable order. The nonrelativistic, infinite-nuclear-mass, atomic Hamiltonian is decomposed in terms of Hylleraas coordinates and spherical harmonics, and the hierarchy of inhomogeneous equations of perturbation theory is solved iteratively. The mixed Hylleraas and Frankowski basis functions are employed to represent accurately the ground-state and perturbed wave functions. We believe our results for nonlinear susceptibilities of helium are the most accurate (and in many cases, the only) available to date, and they are offered as benchmark data for design of future multiphoton experiments. [S1050-2947(97)09111-7]

PACS number(s): 32.80.Rm, 42.65.An, 42.65.Ky, 51.70.+f

I. INTRODUCTION

The high-order nonlinear optical response of noble gases to intense laser radiation is of considerable experimental interest, but is difficult to measure or calculate accurately. To the best of our knowledge, theoretical and experimental data on nonlinear susceptibilities of helium are available only for third and fifth order [1,2]. The theoretical description of these processes is greatly hampered by the nonperturbative nature of the Schrödinger equation in the intense field limit, where nonlinear optical response is strongest, as well as by the notorious difficulty of the quantum-mechanical few-body problem. Moreover, it is difficult to determine reliably from conventional theoretical approximations the thresholds at which perturbative approximations begin to fail, or to predict, in general, the means by which the failures occur.

Most of the theoretical models used so far for strong-field laser-atom interaction employ approximations that reduce the calculation to treat a single active electron. However, most experiments of multiphoton processes are on rare gases, which are easy to handle experimentally, and they are particularly suited for studying the effects of high intensities as their large ionization potentials prevent ionization at low intensities. Due to the presence of six equivalent electrons in the outer subshell of the rare gases (other than helium), comprehensive theoretical treatments for rare gas atoms are very difficult except under the approximation of ''the single-active-electron model'' [3–7].

In the treatment of many-electron atoms, two-electron systems occupy a special position, since they admit the simplest theoretical treatment. In recent years, developments in computational facilities have begun to allow theorists to deal with the time-dependent behavior of two-electron atoms [8–12], though the general case of the few-body time-dependent Schrödinger equation (TDSE) is still at the frontier of the capabilities of modern numerical simulations.

Previous works [13–15] have calculated the ac Stark coefficients and high-order nonlinear susceptibilities of atomic hydrogen within the framework of Rayleigh-Schrödinger perturbation theory at lowest applicable order. This method can be extended to determine the thresholds at which the perturbative approximations begin to fail [15]. In this work, we follow a similar path for helium, to provide a basic description of multiphoton processes in two-electron atoms by accurate calculations of high-order nonlinear susceptibilities within the framework of perturbation theory. With a nonrelativistic treatment, assuming infinite nuclear mass, the atomic Hamiltonian is decomposed in term of Hylleraas coordinates and spherical harmonics using the formalism of Pont and Shakeshaft [16], and the hierarchy of inhomogeneous equations of perturbation theory is solved iteratively.

A combination of Hylleraas and Frankowski basis functions is used [17,18]. The compact Hylleraas basis provides a highly accurate representation of the ground-state wave function, whereas the diffuse Frankowski basis functions efficiently reproduce the correct asymptotic structure of the perturbed orbitals. The use of this mixed basis gives very accurate energies for the ground-state energy and polarizability, and it should account for most effects of electron correlation. The complex rotation scheme has been applied to overcome the difficulty of the boundary condition for continuum solutions.

Our results consist of frequency-dependent susceptibilities $\chi_q(\omega)$, for order q up to 15, for several commonly used laser frequencies. These values are in good agreement with the few experimental and theoretical values that have been reported previously. We also present results for the photoionization cross sections of He for photon energies up to 60 eV. We believe these cross sections have an uncertainty of about 0.1%, based on the convergence behavior observed in the complex-coordinate method.

In the description of the method, we use the conventional system of atomic units, in which the electron charge and mass, and the reduced Planck constant $\hbar = h/2\pi$, have the numerical value of one. Our results for the nonlinear suscep-

*Present address: Rochester Theory Center for Optical Science and Engineering, University of Rochester, Rochester, NY 14627.

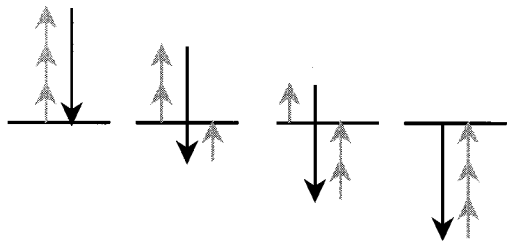

FIG. 1. Path diagrams for χ_3. Each diagram indicates a sequence of virtual photon absorption (↑) and emission (↓).

tibilities χ_q are given in customary electrostatic units (esu) as $\mathrm{cm}^3(\mathrm{cm}^3/\mathrm{erg})^{(q-1)/2}$.

II. METHOD OF COMPUTATION

The task is to compute the atomic nonlinear susceptibility $\chi_q(-q\omega;\omega,\ldots,\omega)$, which is the transition amplitude for an atom in its ground state $|g\rangle$ to absorb q photons of the fundamental frequency ω and to emit one photon of frequency $q\omega$. In lowest-order perturbation theory

$$\chi_q(\omega)=\sum_{k}^{q+1}\sum_{i_1,\ldots,i_q}^{\infty}\frac{d_{gi_q}d_{i_qi_{q-1}}\cdots d_{i_2i_1}d_{i_1g}}{(\omega_{i_qg}-s_{kq}\omega)\cdots(\omega_{i_1g}-s_{k1}\omega)}, \quad (1)$$

where each index i_n runs over the complete atomic spectrum, including the continuum; the index k labels the $q+1$ pathways (see Fig. 1), that represent the distinguishable order of the absorption of incident photons and the emission of the harmonic photon; $d_{ij}=-\langle i|z|j\rangle$ is the matrix element of the dipole operator; $\omega_{ij}=E_i-E_j$ is the energy difference between state i and j; and s_{ij} is a photon number index, that can be defined recursively as

$$s_{k1}=\begin{cases}1 & \text{for } k\neq 1\\ -q & \text{for } k=1,\end{cases}\qquad s_{kj}=\begin{cases}s_{kj-1}+1 & \text{for } k\neq j\\ s_{kj-1}-q & \text{for } k=j.\end{cases} \quad (2)$$

This form of nonlinear susceptibility is difficult to calculate, especially to higher order. There are many summations over infinite intermediate discrete and continuous states and the number of pathways increases very rapidly with order.

The nonlinear susceptibility can be rewritten as

$$\chi_q(\omega)=\sum_{k}^{q+1}\langle g|d|\phi_q^{(k)}\rangle, \quad (3)$$

where $\phi_q^{(k)}$ is a virtual state, described by the qth-order perturbed wave function. This wave function is the solution of the inhomogeneous differential equation of qth-order perturbation theory:

$$(H_a-E_g-s_{kq}\omega)|\phi_q^{(k)}\rangle=d|\phi_{q-1}^{(k)}\rangle, \quad (4)$$

with the initial condition $|\phi_0^{(k)}\rangle=|g\rangle$. H_a in Eq. (4) is the atomic Hamiltonian and E_g is the ground state energy. Here the implicit summation of Eq. (1) is performed by solving the hierarchy of differential equations. In a partial wave representation, this system [Eq. (4)] reduces to a finite set of coupled ordinary differential equations.

When the photon number index s_{ij} is such that $s_{ij}\omega>|E_g|$, the general solution of Eq. (4) is no longer a square-integrable function, and cannot in principle be represented by Hylleraas and Frankowski functions. This corresponds to the situation in which the number of photons absorbed is enough to ionize the atom, so the perturbed wave function is in the continuum. This difficulty can be overcome by using the complex rotation method [14,15]. This method has been applied to calculations of resonances and the Stark effects from the 1960s [19–21], and has been applied to the calculation of nonlinear optical response of atomic hydrogen [15].

The complex rotation scheme invokes the transformation

$$r\rightarrow re^{i\theta},\quad H(r)\rightarrow H(re^{i\theta}) \quad (5)$$

as applied to the composite atom-field Hamiltonian H. Under this transformation, all unbound-state eigenfunctions of H become resonances with complex eigenvalues. These complex eigenvalues have negative imaginary parts, which describe the exponential decay of the resonance states. The wave functions corresponding to these resonances are the so-called Siegert states, which satisfy the outgoing-wave boundary condition and become square integrable after rotation [14,15,21].

The resonance wave function is calculated by applying conventional Rayleigh-Schrödinger perturbation theory to the rotated Hamiltonian and expanding each order of perturbed wave function in the combined Hylleraas and Frankowski functions. Note that, in the case $s_{ij}\omega>|E_g|$, the qth-order perturbed wave function will be a mixture of discrete and outgoing-wave-continuum functions, so this wave function becomes square integrable on complex rotation. In this way, our use of an L^2 basis accounts for continuum-continuum interaction to the relevant order in a consistent manner, within the framework of Rayleigh-Schrödinger perturbation theory.

III. BASIS FUNCTIONS AND DECOMPOSITION OF HELIUM HAMILTONIAN

To obtain highly accurate representations of the initial functions and the perturbed functions, we use a combination [17,18] of Hylleraas functions:

$$\Psi(s,t,u)=s^n t^l u^m e^{-s/2}, \quad (6)$$

and Frankowski functions:

$$\Psi(s,t,u)=s^n t^l u^m e^{-s/2}\times\begin{Bmatrix}\sinh(ct)\\ \cosh(ct)\end{Bmatrix}, \quad (7)$$

in terms of the Hylleraas variables,

$$s=r_1+r_2,\quad t=r_1-r_2,\quad u=r_{12}, \quad (8)$$

where the choice of sinh or cosh depends on the exchange symmetry of the wave function and upon whether l is even or odd, and $|c|\leqslant 1/2$. In the Frankowski basis functions the hyperbolic factor times the $e^{-s/2}$ yields a properly symmetrized sum of products of exponentials with two different parameters, $1/2\pm c$, representing the two different length scales on which the ''inner'' and ''outer'' electrons move in

either the hydrogen ion or a singly excited state of helium. The Frankowski basis functions involving cosh(ct) reduce to the Hylleraas basis functions by setting $c=0$.

It is important to note that these basis functions are nonorthogonal and they are nearly degenerate when the number of basis functions is large. The solution of the ground-state energy and the ground-state wave function of helium is a generalized eigenfunction problem $H|\phi\rangle=N|\phi\rangle$. A Cholesky transformation [22,23] has been used to quasiorthogonalize the basis set. This not only simplifies the generalized eigenfunction problem to the standard eigenfunction problem but also substantially reduces the condition number of the matrices. The normal matrix N is expressed as the product

$$N=LL^T, \tag{9}$$

where L is a lower triangular matrix and all matrices M and wave functions $|\phi\rangle$ are transferred to

$$\widetilde{M}=L^{-1}M(L^T)^{-1}, \quad |\widetilde{\phi}\rangle=L^T|\phi\rangle. \tag{10}$$

Now the standard eigenvalue problem can be solved by the inverse iteration method [22], since only one eigenfunction is needed and the ''exact'' eigenvalue is known.

The nearly degenerate nature of the basis set limits the number of basis functions that can be used, due to roundoff error. With 64-bit arithmetic we can only use up to 250 functions of this type. Most of the calculations reported here use 128-bit arithmetic. The computational speed of the 128-bit arithmetic number is about six to eight times slower than that of 64 bits.

The nonrelativistic, infinite-nuclear-mass, energy of the helium ground state recently obtained by Drake and Yan [24,25] is

$$E=-2.903\ 724\ 377\ 034\ 119\ 5 \ \text{a.u.} \tag{11}$$

This result was obtained using a basis of 1262 functions and an extrapolation procedure to estimate the fully converged result. In the present work, using 215 Hylleraas basis functions including negative powers of s, the ground-state energy is $-2.903\ 724\ 376\ 5$ a.u., accurate to 5×10^{-10} a.u. Although, for the ground state of He^4, the nonrelativistic mass correction is at the order of 10^{-4} and the relativistic correction is at the order of 10^{-5} [25], very accurate nonrelativistic states and energies are still necessary to calculate these corrections. In this work, since the error would increase in each step of iteration, the very accurate ground state and energy are desirable to maintain reasonable accuracy in high-order susceptibilities.

The helium wave function $\phi_q^{(k)}$ is expressed as

$$\phi(\mathbf{r}_1,\mathbf{r}_2)=\sum \psi^L_{l_1,l_2}(s,t,u)|l_1l_2L\rangle, \tag{12}$$

where

$$|l_1l_2L\rangle=\sum_m \langle l_1ml_2(-m)|l_1l_2L0\rangle Y^m_{l_1}(\hat{r}_1)Y^{-m}_{l_2}(\hat{r}_2). \tag{13}$$

For states $l_1+l_2=L$, the helium atomic Hamiltonian can be decomposed to a tridiagonal form using the formalism of Pont and Shakeshaft [16]. Let

$$\Psi^{M=0}_L(\mathbf{r}_1,\mathbf{r}_2)=\sum_{l_1+l_2=L} r_1^{l_1}r_2^{l_2}|l_1l_2L\rangle\psi^L_{l_1,l_2}(s,t,u). \tag{14}$$

Assuming that H_a is the helium Hamiltonian, and H_a^0 is the helium Hamiltonian for wave functions of spherical symmetry,

$$H_a\Psi^{M=0}_L(\mathbf{r}_1,\mathbf{r}_2)=\sum_{l_1+l_2=L} r_1^{l_1}r_2^{l_2}q^L_{l_1l_2}(s,t,u), \tag{15}$$

where

$$\begin{aligned} q^L_{l_1l_2}=H_a^0\psi^L_{l_1,l_2}-\Bigg(&\frac{2(l_1+l_2)s-2(l_1-l_2)t}{s^2-t^2}\frac{\partial}{\partial s}\\ &+\frac{2(l_1-l_2)s-2(l_1+l_2)t}{s^2-t^2}\frac{\partial}{\partial t}+\frac{(l_1+l_2)}{u}\frac{\partial}{\partial u}\Bigg)\psi^L_{l_1,l_2}\\ &+\frac{(l_1+1)}{u}\frac{\partial\psi^L_{l_1+1,l_2-1}}{\partial u}+\frac{(l_2+1)}{u}\frac{\partial\psi^L_{l_1-1,l_2+1}}{\partial u}. \end{aligned} \tag{16}$$

The tridiagonal form can be solved fast and accurately by the efficient tridiagonal algorithm, which plays a vital role in this calculation.

Beginning with the ground state $|l_1=0,l_2=0,L=0\rangle$, the process of the iterative calculation produces not only $|l_1,l_2,L\rangle$ states for which $l_1+l_2=L$ but also $|l_1'l_2'L\rangle$ states for which $l_1'+l_2'>L$. If including $|l_1'l_2'L\rangle$ states, the helium atomic Hamiltonian cannot be decomposed to a tridiagonal form and cannot be solved efficiently. In order to avoid this difficulty, these $|l_1'l_2'L\rangle$ states are projected onto $|l_1l_2L\rangle$ states. This can be done because in general $\langle l_1'l_2'L|l_1l_2L\rangle\neq0$ in the Hylleraas coordinate system [26]. Although the $|l_1'l_2'L\rangle$ states cannot be completely expanded by the $|l_1l_2L\rangle$ states, such procedure allows us to include significant contribution due to the $|l_1'l_2'L\rangle$ states. We have verified such approximation by comparing our results with previous theoretical calculations (see Table III); we find that the results are much better than simply omitting the $|l_1'l_2'L\rangle$ states.

For matrix elements involving states of high angular momentum, the evaluation of angular integrals and the reduction to radial integrals can become very laborious. The problem is complicated by the fact that if s, t, and u are regarded as the independent variables in the radial integration, then only one of $\hat{r}_1$ or $\hat{r}_2$, which are unit vectors for r_1 or r_2, may be treated as independent variables of angular integration. The general reduction of matrix elements to radial integrals over s, t, and u has been studied by several authors [26,27] and their formulations are used to calculate the coupling coefficients between states $|l_1l_2L\rangle$.

IV. FREQUENCY-DEPENDENT POLARIZABILITIES OF HELIUM

The frequency-dependent polarizability $\alpha(\omega)$ is an important quantum-mechanical property which has been evaluated

TABLE I. Frequency-dependent polarizabilities for the ground state of helium (in a.u.) for frequencies up to the first excitation threshold.

Frequency ω	Polarizability $\alpha(\omega)$
0.0	1.38319194
0.05	1.38706008
0.1	1.39882036
0.15	1.41895763
0.2	1.44834178
0.25	1.48833549
0.3	1.54098157
0.35	1.6093254
0.4	1.6979853
0.45	1.8142153
0.5	1.9700396
0.55	2.1870030
0.6	2.508364
0.65	3.037843
0.7	4.11614
0.75	8.1750

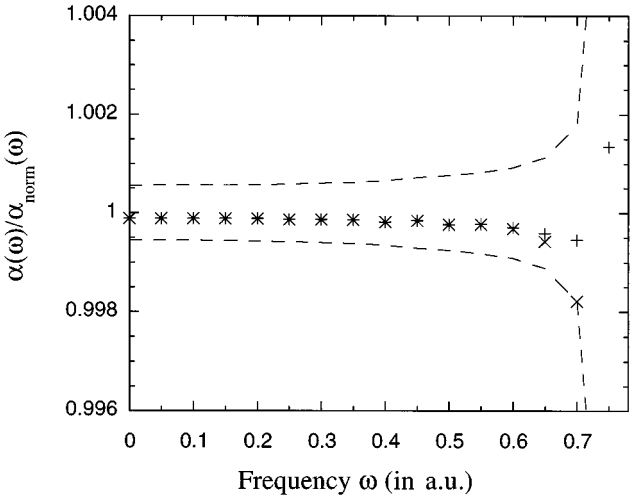

FIG. 2. Frequency-dependent polarizabilities of the ground state of helium for frequencies ω up to the first excitation threshold, expressed relative to the mean of the rigorous upper and lower bounds of Glover and Weinhold's work. Dashed lines are Glover and Weinhold's rigorous bounds [29]. + denotes the results of present work. × denotes the results of Bishop and Lam [30]. When $\omega = 0.75$ a.u., Bishop and Lam's result is out of the rigorous bound.

by numerous theoretical techniques. Dalgarno [28] has reviewed the earlier theoretical literature. In a milestone paper, Glover and Weinhold [29] gave rigorous upper and lower bounds of dynamic polarizabilities of two-electron atoms. Recently, Bishop and Lam [30] published more accurate results (especially for lower frequencies) for the dynamic polarizabilities of helium.

When the field frequency goes beyond the ionization threshold, the atom or molecule is ionized and the polarizabilities carry an imaginary part which is related to the photoionization cross section. Since the first calculation of the helium cross section by Wheeler [31], helium has attracted considerable attention because of its importance as a testing ground for theory. In the last few years, numerous calculations of the helium photoionization cross section have made use of a variety of sophisticated methods, many of which give cross section values within 1–4 % of each other. Samson *et al.* [32] have reviewed recent theoretical and experimental results and provide critically evaluated cross section data with an absolute uncertainty of $\pm 1\%$ to $\pm 1.5\%$ from threshold to about 60 eV and of $\pm 2\%$ from 60 to 120 eV. Our calculations on the frequency-dependent polarizabilities can be compared to the experiments to test the validity of our methods.

We calculate the frequency-dependent polarizabilities of helium as the first-order susceptibilities. In this calculation, we use a basis set with 385 basis functions for each $|l_1 l_2 L\rangle$ with optimal parameter c in Frankowski basis functions.

For the dc case ($\omega = 0$), we obtain the polarizability $\alpha(0) = 1.383\,191\,94$ a.u. This is to be compared to the result from Bishop and Lam, 1.383 192 a.u. [30], and the very accurate result from Bhatia and Drachman, 1.383 192 179 3 a.u. [33]. The agreement is within 2×10^{-7} a.u.

For laser frequencies less than the first ionization threshold, the results of our calculations are shown in Table I. In Fig. 2, the results of present work are compared with Glover and Weinhold's rigorous bounds and Bishop and Lam's results. For frequencies up to the first excitation threshold, our calculations agree with Glover and Weinhold's rigorous bounds quite well, but for the regime between the first and second excitation thresholds, there are some differences. As commented in Glover and Weinhold's paper, the Hylleraas-like formulation we used is not suitable to produce optimal results in this regime.

For laser frequencies above the first ionization threshold, the polarizabilities are complex. The imaginary part of the polarizability corresponds to the photoionization rate and the photoionization cross section σ is

$$\sigma = (4\pi\omega/c)\,\mathrm{Im}[\alpha]. \tag{17}$$

We analyze the θ trajectories of complex rotation calculations to determine the stationary values of complex polarizabilities [20]. The typical trajectories are shown in Fig. 3. The trajectories that pause near certain values of θ suggest some sort of stationary property. The approximate stationary point, easily observed in the figure, determines the position of the complex polarizability within an uncertainty of about 10^{-3}.

Our calculations (see Table II) agree well with the experimental results of Samson *et al.* [32]. The results show that the complex rotation method combined with the mixed basis function can represent perturbative wave functions, even when the frequency is above the ionization threshold.

V. HIGH-ORDER SUSCEPTIBILITIES

There are few theoretical calculations and experiments on frequency-dependent high-order susceptibilities of helium. The calculations of nonlinear susceptibilities (hyperpolarizabilities) for complex atoms have been limited to the first order. Manakov and Ovsyannikov [2] have calculated up to

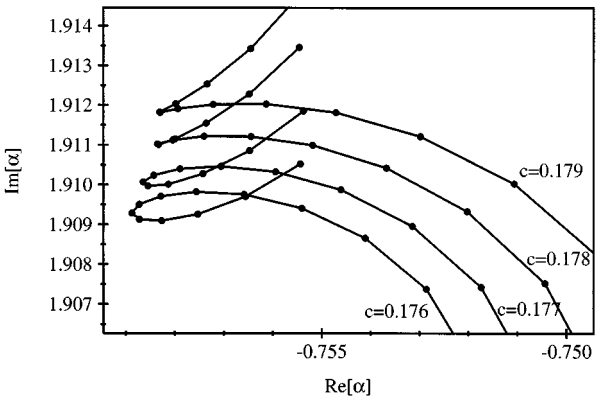

FIG. 3. θ trajectories for the location of the complex polarizabilities for the ground state of helium. Frequency is 1.102 47 a.u.=30 eV. Trajectories show behavior of complex polarizabilities as a function of the complex scaling angle θ, for four different parameters c of the Frankowski basis functions. Each point represents an equal-step change of $\Delta\theta=0.02$.

the fifth-order susceptibility of helium for the Nd:YAG (YAG denotes yttrium aluminum garnet) laser frequency, using a model potential obtained by fitting the discrete energies to the experimental spectrum and Green's function techniques for the summations. Bishop and co-workers [30,34] used an *ab initio* method to calculate third-order nonlinear optical properties of helium using the formula of Eq. (1) to get more accurate results. A comparison of their calculations and this work is shown in Table III. Our result is close to that of Bishop and co-workers and falls within the uncertainty of the experiments.

With Green's function techniques or the pseudosummation method, it is very difficult to go to higher order. On the other hand, the iterative solutions can be extended to higher order. Table IV and Fig. 4 show high-order susceptibilities at various wavelengths. In this work, we use a basis set with 307 basis functions for each $|l_1 l_2 L\rangle$; the set includes 56 Hylleraas type functions, including negative powers of s, and 251 Frankowski type functions.

In the case of $\lambda=248$ nm, 5ω is larger than the ionization threshold and we must use the complex rotational scheme to calculate high-order susceptibilities. The θ trajectories of χ_5 are similar to the θ trajectories of the polarizabilities. The values of complex susceptibilities are $\chi_5=(2.15+5.07i)\times10^4$, $\chi_7=(2.2+0.6i)\times10^6$, and $\chi_9=(4.5+5i)\times10^7$ (in a.u.).

The behavior of susceptibilities can be better quantified in terms of critical intensities [35]. The critical intensity for the qth harmonic, $I_c(q)$, is defined as the intensity of the incident laser at which the intensity of the $(q+2)$th harmonic becomes equal to the qth. Within the perfect phase-matching assumption or, equivalently, in a single-atom picture, this critical value is

$$I_c(q)=\frac{c}{2\pi}\frac{q}{q+2}\left|\frac{\chi_q}{\chi_{q+2}}\right|. \tag{18}$$

Obviously, the relative harmonic intensities decrease monotonically when the intensity of the incident light is lower than the lowest I_c and increase monotonically when the incident laser intensity is higher than the highest I_c. For intermediate incident intensities, nonmonotonic relative intensity, or plateau regions, will appear.

Figure 5 shows the critical intensities at various laser wavelengths. As in previous calculations on atomic hydrogen [14,15], when all the virtual states are below the ionization threshold, I_c tends to decrease as a function of harmonic order. This trend is changed when the virtual states go above threshold, as in the case of wavelength $\lambda=248$ nm.

TABLE II. Polarizabilities and photoionization cross sections of helium for photon energies above the first ionization threshold.

Photon energy (in eV)	Polarizability (in a.u.)	Cross section (in Mb) present work	Cross section (in Mb) Samson *et al.* [32]
27	$-0.57+2.52i$	6.42	6.40
30	$-0.758+1.911i$	5.410	5.38
35	$-0.809+1.242i$	4.102	4.09
40	$-0.739+0.843i$	3.182	3.16
45	$-0.645+0.594i$	2.522	2.48
50	$-0.555+0.433i$	2.043	2.02
55	$-0.473+0.326i$	1.692	1.67
58	$-0.426+0.288i$	1.576	1.58

VI. EFFECTS OF ELECTRON CORRELATION

We can apply the independent-electron (IE) model [36–38] to describe helium. Comparing the results from the IE model and our calculations, which include full electron correlation effects, we can obtain a better understanding of the effects of electron correlation.

We assume the model of the helium atom in which the two electrons are independent. This is equivalent to the replacement of $1/r_{12}$ in the atomic potential by some screening modification in the $-2/r$ potential experienced by each electron, which allows the quantum description to be modeled by two independent electrons that each experience only some effective potential $V(r)$. A well-known model of a separable helium atom is that corresponding to the single-exponential variational ground-state wave function $\exp[-Z(r_1+r_2)]$, with $Z=27/16$. The reduction of the effective charge Z from the

TABLE III. Susceptibilities $|\chi_q|$ (in esu) of helium at wavelength $\lambda=1064$ nm (Nd:YAG laser). (a) Manakov and Ovsyannikov [2]; (b) Bishop and Pipin [34]; (c) Li *et al.* [41]; (d) Lehmeier *et al.* [42].

q	This work	Theory (a)	Theory (b)	Expt. (c)	Expt. (d)
3	3.7768×10^{-39}	4.86×10^{-39}	3.7986×10^{-39}	3.7×10^{-39}	3.6×10^{-39}
5	2.671×10^{-52}	4.97×10^{-52}			

TABLE IV. Susceptibilities $|\chi_q|$ (in esu) of helium at commonly used laser wavelengths.

q	$\lvert\chi_q\rvert$ $\lambda \approx 46\ \mu$m (low frequency limit)	$\lvert\chi_q\rvert$ at 1064 nm	$\lvert\chi_q\rvert$ at 532 nm	$\lvert\chi_q\rvert$ at 248 nm
1	2.04968×10^{-25}	2.05388×10^{-25}	2.06661×10^{-25}	2.13042×10^{-25}
3	3.68886×10^{-39}	3.7768×10^{-39}	4.50293×10^{-39}	1.13683×10^{-38}
5	2.16175×10^{-52}	2.7640×10^{-52}	6.2491×10^{-52}	9.43×10^{-50}
7	2.2140×10^{-65}	4.64×10^{-65}	6.486×10^{-64}	1.3×10^{-62}
9	3.2299×10^{-78}	1.71×10^{-77}	8.51×10^{-74}	1.3×10^{-75}
11	5.85×10^{-91}	1.33×10^{-89}		
13	1.19×10^{-103}	2.2×10^{-101}		
15	2.53×10^{-116}	9.3×10^{-113}		

value of 2 is a measure of the mutual radial screening of the electrons and so the use of this IE model includes some of the effects of the electron-electron interaction. This model gives a total binding energy that is within 2% of the exact value for ground-state helium. It seems to be a reasonable first approximation to take.

Pan *et al.* have calculated high-order susceptibilities of hydrogenic ions using the same perturbation theory scheme applied in this work [14]. Taking the susceptibilities of He^+ at Nd:YAG laser frequency $\omega = 0.0428$ a.u., we can use these data and transfer them to high-order susceptibilities of a hydrogenic ion of effective charge $Z = 27/16$ by the scaling rule [14]

$$\chi_q(Z,\omega) = (Z/Z_0)^{-(3q+1)}\chi_q[Z_0, \omega(Z/Z_0)^{-2}]. \quad (19)$$

In the case of He^+, $Z_0 = 2$. The frequency after scaling is 0.030 48 a.u. ($\lambda = 1494$ nm). Multiplying the susceptibilities of hydrogenic ion of effective charge $Z = 27/16$ by 2 for there are two independent electrons, we obtain the susceptibilities of the IE model, shown in Fig. 6 with the nonlinear susceptibilities of helium. The critical intensities for both cases are shown in Fig. 7. The critical intensities have similar tendencies but our calculations give higher values. The difference between these two results increases with increasing harmonic order. The χ_1 and χ_3 are of the same order, but the susceptibilities differ more with increasing harmonic order. We can conclude that electron correlation contributes significantly to higher-order optical processes.

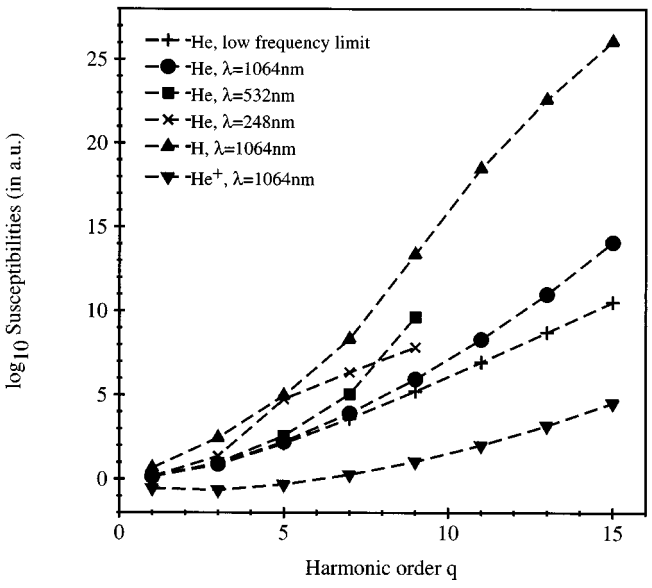

FIG. 4. Susceptibilities $|\chi_q|$ (in a.u.) of helium and hydrogen at commonly used laser wavelengths. The data for H and He^+ are from Pan *et al.* [14,15].

VII. DISCUSSION AND CONCLUSION

Our results compared with the IE model indicate that electron correlation plays a substantial role in high-order processes. Further comparison with the results from more sophisticated single-active-electron models (for example, the work by Kulander and co-workers [39,7,3–5]) or the models including partial electron correlation (for example, the work by Blodgett-Ford *et al.* [9]) should give more insight into this important issue.

Kulander and co-workers [39] have calculated the harmonic intensities for helium at 527 nm and laser intensities of $(1-6)\times10^{14}$ Wcm^{-2}. The spectra all show that intensities of the first several harmonics decrease monotonically, but the ninth harmonic is stronger than the seventh. Our calculations at 532 nm (see Fig. 5) show $I_c(7)$ is less than 10^{14} Wcm^{-2}, which agrees with their results. On the other

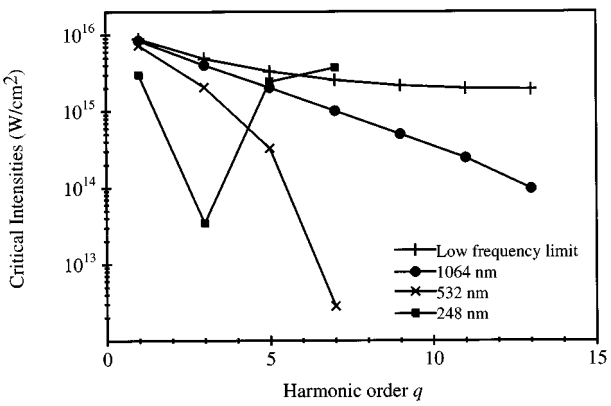

FIG. 5. Critical intensities of helium at commonly used laser wavelengths.

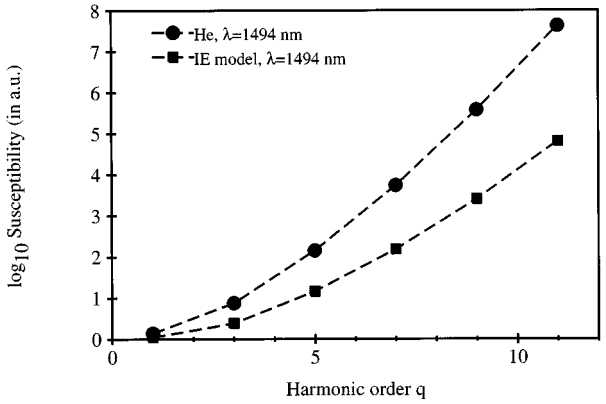

FIG. 6. Susceptibilities $|\chi_q|$ (in a.u.) of helium and of the IE model at wavelength equal to 1494 nm.

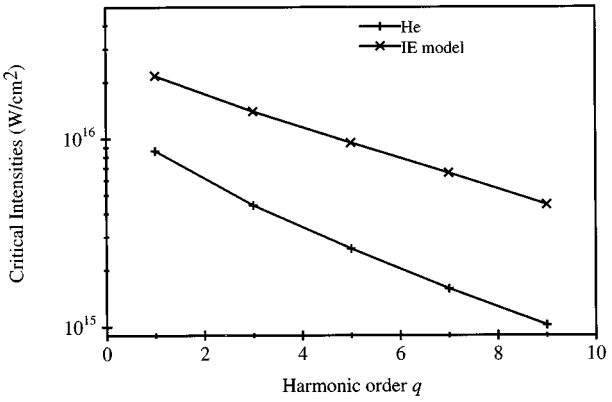

FIG. 7. Critical intensities of helium and of the IE model at wavelength equal to 1494 nm.

hand, $I_c(5)\approx 3.3\times 10^{14}$ Wcm^{-2} is not consistent with their spectra with higher laser intensities.

Xu *et al.* [40] have solved the TDSE for helium on a numerical grid with a model potential. The basic idea of the model potential method is to freeze one electron in its ionic ground state and to treat the motion of the second electron in the presence of the ion core by a model potential with several free parameters. The parameters of the model potential are adjusted to fit the data from experiments or other well-established theoretical calculations. The harmonic spectra have been calculated for a photon energy of 5.0 eV ($\approx$0.1837 a.u., corresponding to $\lambda = 248$ nm) at the intensity $I=6\times 10^{14}$ Wcm^{-2}. In the results of Xu *et al.*, the fifth harmonic is stronger than the third harmonic, the seventh harmonic is weaker than the fifth, and the ninth harmonic is weaker than the seventh. These results agree well with our calculations, $I_c(3)<I=6\times 10^{14}$ Wcm$^{-2}<I_c(5),I_c(7)$ for frequency equal to 248 nm (see Fig. 5).

In this work we have calculated nonlinear susceptibilities χ_q of helium at various commonly used laser frequencies from lowest-order perturbation theory up to $q=15$. These results are the first accurate *ab initio* quantum-mechanical calculations for high-order ($q>5$) susceptibilities of helium. In spite of the rapid development in the theoretical study of intense-field laser-atom interactions, perturbation theory remains perhaps the best-established and best-understood theoretical approach. We believe that these quantitative results of perturbative studies of helium provide a solid ground for specific identification of the onset of nonperturbative behavior and for the necessary development of a corresponding theory.

To have a quantitative evaluation of the limitations of perturbation theory, the next natural step is to calculate the next-lowest-order term in the perturbative expansion of χ_q. This requires a great amount of computational work. In the case of atomic hydrogen [15], the next-lowest-order term helps to define an upper bound to the intensities for which lowest-order perturbation theory may be expected to give reliable predictions for the qth-order process. For atomic hydrogen at the Nd:YAG laser frequency, the results show that for intensities as low as 10^{11} Wcm^{-2}, lowest-order perturbation theory is no longer valid for 11th- to 29th-order processes. For helium, we expect the limit should be higher due to the higher ionization threshold. It is important to know the location of the boundary of validity of the lowest-order perturbation theory for helium.

ACKNOWLEDGMENTS

I would like to thank my advisor C. W. Clark for his guidance and valuable discussion through this work. He proposed the use of a mixed basis set to achieve high accuracy results. This research and computational facilities are supported by National Institute of Standards and Technology.

[1] A. L'Huillier, L. A. Lompré, G. Mainfray, and C. Manus, in *Atoms in Intense Laser Fields*, edited by M. Gavrila (Academic Press, Boston, 1992).

[2] N. L. Manakov and V. D. Ovsyannikov, Zh. Éksp. Teor. Fiz. **79**, 1769 (1980) [Sov. Phys. JETP **52**, 895 (1980)].

[3] K. C. Kulander, Phys. Rev. A **36**, 2726 (1987).

[4] K. C. Kulander and B. W. Shore, Phys. Rev. Lett. **62**, 524 (1989).

[5] K. C. Kulander and B. W. Shore, J. Opt. Soc. Am. B **7**, 502 (1990).

[6] K. Kulander, K. J. Schafer, and J. L. Krause, in *Atoms in Intense Laser Fields*, edited by M. Gavrila (Academic Press, Boston, 1992).

[7] K. C. Kulander, K. J. Schafer, and J. L. Krause, in *Super-Intense Laser-Atom Physics*, Vol. 316 of *NATO Advanced Study Institute, Series B: Physics*, edited by B. Piraux, A. L'Huillier, and K. Rzążewski (Plenum Press, New York, 1993), p. 95.

[8] J. Purvis *et al.*, Phys. Rev. Lett. **71**, 3943 (1993).

[9] S. Blodgett-Ford, J. Parker, and C. W. Clark, in *Super-Intense Laser-Atom Physics*, Vol. 316 of *NATO Advance Study Institute, Series B: Physics*, edited by B. Piraux, A. L'Huillier, and

K. Rzążewski (Plenum Press, New York, 1993).
[10] M. Horbatsch, Z. Phys. D **30**, 31 (1994).
[11] J. Zhang and P. Lambropoulos, J. Phys. B **28**, L101 (1995).
[12] J. Parker, K. T. Taylor, C. W. Clark, and S. Blodgett-Ford, J. Phys. B **29**, L33 (1996).
[13] L. Pan, K. T. Taylor, and C. W. Clark, Phys. Rev. Lett. **61**, 2673 (1988).
[14] L. Pan, K. T. Taylor, and C. W. Clark, Phys. Rev. A **39**, 4894 (1989).
[15] L. Pan, K. T. Taylor, and C. W. Clark, J. Opt. Soc. Am. B **7**, 509 (1990).
[16] M. Pont and R. Shakeshaft, Phys. Rev. A **51**, 257 (1995).
[17] J. D. Baker, Master's thesis, University of Delaware, 1988.
[18] J. D. Baker, R. N. Hill, and J. D. Morgan, in *Relativistic, Quantum Electrodynamic, and Weak Interaction Effects in Atoms*, edited by W. Johnson, P. Mohr, and J. Sucher, AIP Conf. Proc. No. 189 (AIP, New York, 1989), p. 123.
[19] C. Cerjan *et al.*, Int. J. Quantum Chem. **14**, 393 (1978).
[20] W. P. Reinhardt, Annu. Rev. Phys. Chem. **33**, 223 (1982).
[21] B. R. Junker, Adv. At. Mol. Phys. **18**, 207 (1982).
[22] W. H. Press, B. P. Flannery, S. A. Teukolsky, and W. T. Vetterling, *Numerical Recipes* (Cambridge University Press, Cambridge, England, 1986).
[23] G. H. Golub and C. F. V. Loan, *Matrix Computations*, 2nd ed. (Johns Hopkins University Press, Baltimore, 1989).
[24] G. W. F. Drake and Z.-C. Yan, Chem. Phys. Lett. **229**, 486 (1994).
[25] G. W. F. Drake, in *Atomic, Molecular & Optical Physics Handbook*, edited by G. W. F. Drake (AIP Press, New York, 1996).
[26] G. W. F. Drake, Phys. Rev. A **18**, 820 (1978).
[27] J.-L. Calais and P.-O. Löwdin, J. Mol. Spectrosc. **8**, 203 (1963).
[28] A. Dalgarno, Adv. Phys. **11**, 281 (1962).
[29] R. M. Glover and F. Weinhold, J. Chem. Phys. **65**, 4913 (1976).
[30] D. M. Bishop and B. Lam, Phys. Rev. A **37**, 464 (1988).
[31] J. A. Wheeler, Phys. Rev. **43**, 258 (1933).
[32] J. A. R. Samson, Z. X. He, L. Yin, and G. N. Haddad, J. Phys. B **27**, 887 (1994).
[33] A. K. Bhatia and R. K. Drachman, J. Phys. B **27**, 1299 (1994).
[34] D. M. Bishop and J. Pipin, J. Chem. Phys. **91**, 3549 (1989).
[35] J. F. Reintjes, *Nonlinear Optical Parametric Processes in Liquids and Gases* (Academic, New York, 1984).
[36] S. Geltman, Phys. Rev. Lett. **54**, 1909 (1985).
[37] S. Geltman and J. Zakrzewski, J. Phys. B **21**, 47 (1988).
[38] S. Geltman, Phys. Rev. A **52**, 2468 (1995).
[39] J. L. Krause, K. J. Schafer, and K. C. Kulander, Phys. Rev. Lett. **68**, 3535 (1992).
[40] H. Xu, X. Tang, and P. Lambropoulos, Phys. Rev. A **46**, R2225 (1992).
[41] X. F. Li *et al.*, Phys. Rev. A **39**, 5751 (1989).
[42] H. J. Lehmeier, W. Leupacher, and A. Penzkofer, Opt. Commun. **56**, 67 (1985).